Research Article

Aleksandra A. Belik, Anna A. Kokoreva, Andrei G. Bolotov, Aleksandr V. Dembovetskii, Victoria N. Kolupaeva*, Dmitry V. Korost, Alexei N. Khomyak

Characterizing macropore structure of agrosoddy-podzolic soil using computed tomography

https://doi.org/10.1515/opag-2020-0080
received June 30, 2020; accepted September 23, 2020

Abstract: The agrosoddy-podzolic soil (Eutric Albic Glossic Retisol (Abruptic, Loamic, Aric, Cutanic)) is typical for Moscow Oblast and is used for agricultural purposes, resulting in use of various agrochemicals and pesticides. The presence of macropores and cracks in such soils leads to preferential water and substance transfer and nonequilibrium conditions. Therefore, it is important to study the numerical characteristics of the pore space of soils to adjust mathematical models of substance transfer. Undisturbed soil monoliths 10 cm in diameter taken from Ap (from 0 to 30 cm) and E, BE horizons (from 30 to 50 cm) were investigated under the field moisture conditions and after saturation using the tomographic core analyzer RKT-180 with the resolution of 200 μm/pixel. Using the X-ray computer tomography, it has been established that the plough layer of the agrosoddy-podzolic soil contains over 7% of macropores larger than 1 mm, while the subsurface layer has a porosity of about 3%. After saturation, some of the inter-aggregate pores overlap, which leads to a decrease in the total porosity to 4% in the upper and 2% in lower horizons, as well as increase in the average pore diameter. The number of macropores determined by tomographic analysis is one third higher than the values calculated using pedotransfer functions for this soil. The data obtained in this paper are recommended for use in national scenarios of migration of substances (pesticides, agrochemicals, salts) in soils.

Keywords: X-ray CT, preferential flows, soil pore space, agrosoddy-podzolic soil

*** Corresponding author: Victoria N. Kolupaeva,** Lab of Environmental Chemistry, Russian Scientific-Research Institute of Phytopathology, Bolshiye Vyazemy, Moscow Region, Russia, e-mail: v.kolupaeva@vniif.ru, amulanya@gmail.com
Aleksandra A. Belik: Lab of Environmental Chemistry, Russian Scientific-Research Institute of Phytopathology, Bolshiye Vyazemy, Moscow Region, Russia, e-mail: belikalexandra@gmail.com
Anna A. Kokoreva: Lab of Environmental Chemistry, Russian Scientific-Research Institute of Phytopathology, Bolshiye Vyazemy, Moscow Region, Russia; Faculty of Soil Science, Lomonosov Moscow State University, Moscow, Russia; Institute of Forestry, Russian Academy of Sciences, Uspenskoe, Moscow region, Russia, e-mail: kaa@penreg.ru
Andrei G. Bolotov: Faculty of Agronomy and Biotechnology, Russian State Agrarian University – Moscow Timiryazev Agricultural Academy, Moscow, Russia, e-mail: agbolotov@gmail.com
Aleksandr V. Dembovetskii: Faculty of Soil Science, Lomonosov Moscow State University, Moscow, Russia
Dmitry V. Korost, Alexei N. Khomyak: Faculty of Geology, Lomonosov Moscow State University, Moscow, Russia

1 Introduction

The pore space of soils has a complicated structure including water-conducting paths of various sizes and forms. Depending on their morphological characteristics, pores can be draining elements, store available soil water and nutrients, or contain unavailable water (Ivanov et al. 2019). From the last mid-century, the pore geometry as well as its influence on migration processes was actively studied; these studies discovered that the highest movement velocity is observed in pore centers, while the lowest one – at their walls, due to the influence of the solid phase (Voronin 1986; Shein 2005). Round pores conduct water better than irregular pores, which, in their turn, better retain water (Yang et al. 2018). Thus, the bigger and more round a pore is, the less important sorption forces are and the faster filtration is; that is why, it is important to study large soil pores to control water quality and, for example, to manage pesticides.

Different pore classifications according to their sizes are available (Brewer 1964; Rowell 1998; Capowiez et al. 2011). Macropores and soil conduits can be caused by bioactivities (root paths and worm holes), geological forces (freezing and defrosting, swelling and shrinkage), or agrotechnical activities (Jarvis 2007). The circulation of matters in macropores is much more intensive, due to the good aeration and incoming nutrients (Kuzyakov and Blagodatskaya 2015), besides macropores are paths for the preferential flows in soils. The front of a substance migration is not a uniform chromatic flow, and the movement of water and substances occurs through soil

Open Access. © 2020 Aleksandra A. Belik *et al.*, published by De Gruyter. This work is licensed under the Creative Commons Attribution 4.0 International License.

macropores and cracks. In well-structured heavy-textured soils, cracks and channels usually form less than 1% of the total volume of pores (Tuller and Or 2002). However, during abundant rainfalls, water will mostly flow along these migration paths (Smetnik et al. 2005).

Two types of macropores can be distinguished: (1) open-ended macropores, through which water quickly penetrate underlying horizons, and (2) dead-ended macropores, where the quick transmission of substances to a certain depths changes to the interaction of a solution with a soil matrix (Kordel and Klein 2006). If soils are saturated (durable abundant rainfalls), in spite of a flow in macropores, equilibrium conditions for solving of substances will be observed (Jarvis et al. 2016). However, another situation is more often: the quick flow through the preferential paths causes the nonuniform soil watering; the solution penetrates the soil to a significant depth, almost without interactions with the surrounding soil matrix and beyond the most pore space of the soil (stagnant zone) (Simunek et al. 2003). As a consequence, in structured soils, sorption and degradation processes are much less important for the migration of chemicals. A significant contribution to the movement of moisture is made by soil compaction and its hydrophysical properties, which have significant spatial variability (Simsek et al. 2019; Bolotov et al. 2019; Belik et al. 2019). These conditions are behind the nonequilibrium character of the preferential migration of substances under unsaturated conditions: due to high migration rates, the solution cannot be balanced between a circulation zone and a stagnant zone (Simunek et al. 2003; Jarvis 2007; Jarvis et al. 2016).

The nonequilibrium character of the preferential transport can be simulated using two approaches: physical or chemical (Simunek and van Genuchten 2008). According to the physical approach, preferential flows can be described using dual-porosity models or dual-permeability models and models which combine two above types (Simunek et al. 2003). Dual-porosity models divide pore space into macropores, through which solution moves, and a matrix (intra-structure pores, soil matrix), a "stagnant zone," where the exchange with moving solution occurs (Simunek and van Genuchten 2008). The main differences of dual-permeability models are available transport processes in intra-structure space. Thus, to study and simulate the migration of substances, a pore distribution by sizes as well as characteristics of these migration paths is of great importance.

Nowadays, the most helpful study method used for pore space of soils is the X-ray computer tomography. This method allows studying of undamaged pore space under any watering. Till now, popular methods used to study morphological structure of soils included analyzing of thin soil sections and soil fracture faces using optical and electronic microscopes (Gerke et al. 2012), as well as monitoring of dye traveling to determine paths of solution migration in soils (Shein et al. 2018). However, all the previous methods are destructive; besides, due to the variability of pore space and small scope of the study, a required number of samples can be up to 100 thin sections (Skvortsova et al. 2015), and experiments with field watering are impossible during monitoring of dye traveling. In addition, the X-ray computer tomography can be used to determine single and combined pores, which cannot be determined using soil-water retention methods (Cercioglu 2018). The computer tomography was first used to study large biopores at the end of the last century (Ringrose-Voase 1987; Peyton, et al. 1994). In Russia, tomographic soil studies are actively carried out by a team including scientists from the Dokuchaiev Soil Institute and Geological Faculty of the Lomonosov Moscow State University (Abrosimov et al. 2019; Skvortsova et al. 2020). Globally, the computer tomography is used to study pore space of soils, e.g., some recent papers were dedicated to the assessment of the responses of soil pore properties to combined soil structure amendments (Yang et al. 2018), separation of soil macropore types (Leue et al. 2019), or soil pore structure changes under wetting and drying cycles (Pires et al. 2020; Mady and Shein 2020).

When a tomographic analysis is not an independent study, but is additionally applied to determine physical parameters of soil, an initial condition of a sample becomes important. Thus, for filtration experiments involving soil monoliths, saturation watering (Umarova 2011) is recommended; pore distribution by their sizes is also recommended for initially saturated sample during its further drying (Umarova et al. 2014). Nevertheless, parameters of pore space, which are used for mathematic modeling, are given as averaged values of a whole sample (Beulke et al. 2002). That is why, the issue of pore space changing under different watering conditions and changing of its geometry and quantitative characteristics is important. The purpose of this paper is to study the macroporosity of agrosoddy-podzolic soil monoliths by tomographic method at saturated and unsaturated moisture for the adaptation (provision) of mathematic models of moisture and substance transport.

2 Materials and methods

To study pore space, agrosoddy-podzolic soil (Eutric Albic Glossic Retisol (Abruptic, Loamic, Aric, Cutanic))

(WRB 2014) was selected, which is typical for Moscow region and has preferential migration paths. Samples were taken at the permanent station of the Dokuchaiev Soil Institute in Puskino Raion, Moscow Oblast (56°08′ 01.6″N 37°48′06.8″E). This area is located within the southern slope of Klinsko-Dmitrovskaia ridge included into Smolensk-Moscow Upland and has a gently rolling terrain and the climate (SHishova and Vojtovich 2002). Major parent materials are covering slits with underlying moraine loams or Moscow glaciation clays. A field, which was selected for sampling, had been plowed up for a long time, but in several last years was used for haying only.

Major properties of soil horizons are given in Table 1. Undisturbed soil monoliths were taken from Ap (from 0 to 30 cm) and E, BE horizons (from 30 to 50 cm). Totally, 4 monoliths 10 cm in diameter were taken: two 30 cm high and two 20 cm high monoliths. The samples were tightly packed to prevent their drying.

Monoliths were analyzed using a tomographic core analyzer RKT-180 (Geological Faculty of the Lomonosov Moscow State University, Moscow) with the resolution of 200 μm/pixel, which allowed identification of pore sizes over 1 mm; according to Rowell (1998), these pores are macropores and transport up to 90% of water and substances in soil. RKT-180 was designed to analyze rocks, soils, nonconsolidated bottom sediments, and biological samples and allows three-dimensional distribution of X-ray absorption values of the whole sample volume, within the available resolution. The tomograph operating space is 100 × 100 × 1,000 mm; thus, the whole volume of the selected monoliths could be studied. Each sample included from 1,400 (for 0–30 cm monoliths) to 2,400 (for 30–50 cm monoliths) scanned layers. First, the monoliths were tomographically analyzed under unsaturated conditions (field watering), and then they were capillary-saturated on a sandy bed and re-scanned. This design of the study allowed determining macropores, which were active under unsaturated conditions, i.e., when storm rainfalls came after a drought, and to compare data with pore space under saturated conditions, during long rainfalls. For further analyzing, two-dimensional scans of soil slices (2D analysis) and three-dimensional pore space models (3D analysis) were used. The first step included the binarization of scans; then, special programs developed to process tomographic scans were used for quantitative analysis (DataViewer for vertical sections of soil monoliths, CTAn, CTVol, CTVox for the pore space structure, 3D analysis). The last step included calculations of pore space parameters (morphometrical parameters: total, open and closed pores, pore space adhesion (for monoliths), number of pores) in Excel 2016.

Table 1: Some physical and chemical properties of agrosoddy-podzolic soil

Parameter	Horizon			
	Ap	E	BE	Bt
Depth/ thickness, cm	0–36/36	36–42/6	42–51/9	51–80/29
Total carbon, %	1.07	0.26	0.23	0.22
pH	6.52	6.29	6.07	5.66
Bulk density, g/cm^3	1.20	1.35	1.28	1.43
Particle density, g/cm^3	2.60	2.78	2.72	2.72
Porosity, cm^3/cm^3	0.54	0.51	0.53	0.47
Particle-size composition				
Clay (<2 μm)	10.6	5.2	10.4	12.7
Silt (2–50 μm)	87.9	93.5	89.0	87.3
Sand (>50 μm)	1.5	1.3	0.6	0.0
Saturated hydraulic conductivity, m/day	0.143	0.137	0.428	0.376

We shall note that pore space was tomographically analyzed using large monoliths; this allowed to use the tomographic scanner with a small resolution, and thus, values provided for pore space characteristics are computed values. Besides, it shall be explained that parameters determined based on tomographic scans are horizontal or vertical projections of actual pores. If a pore is located at a certain angle to a projection section, this is the object of computations (Figure 1). Since pores determined in the tomographic scans are 1 mm and more, the total volume of the determined pores can be defined as a total volume of soil macropores or calculated porosity. Remaining space in tomographic scans is defined as a calculated solid phase. However, we shall understand that it includes the solid phase of soil as such and all the pores are under 1 mm, which cannot be determined in tomographic scans (Figure 1).

Below, the definitions of the calculated porosity and the calculated solid phase will be used in this article, while monoliths will be designated as 0–30 (1), 0–30 (2), 30–50 (1), and 30–50 (2) cm, where figures before parentheses are used for monolith depths, while figures in parentheses – for monolith numbers.

We shall note that, after their saturation and tomographic scanning, these soil monoliths were used for filtration experiments involving a marker substance. These studies have been published before and also include the determination of physical parameters of soil pore space, which are required for the further mathematic modeling of water/salt transport in soils (Shein et al. 2018).

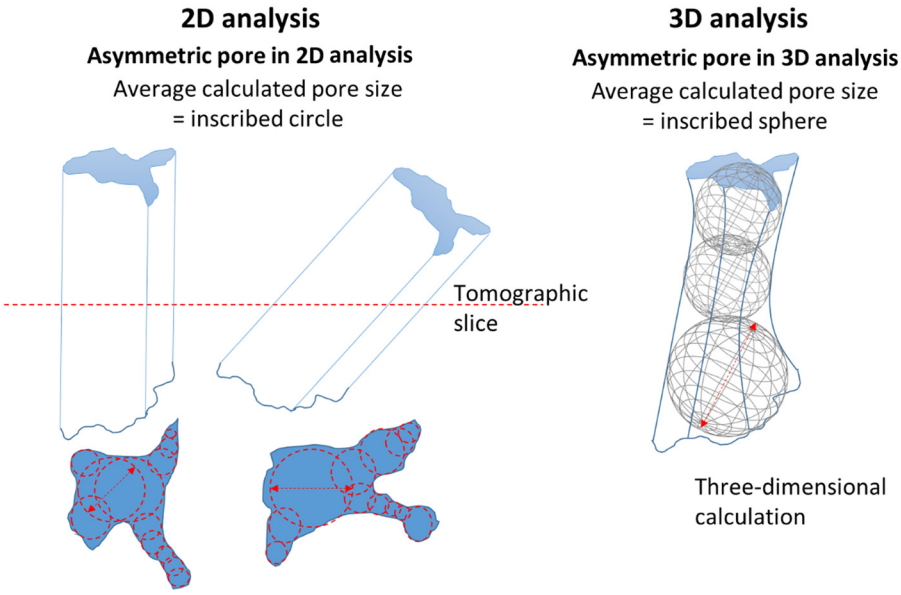

Figure 1: Calculated morphometric parameters of soil pore space.

3 Results and discussion

Figure 2 shows scans of soil monoliths in different projections, a general image for unsaturated conditions, and separate scans for comparing monoliths before and after saturation. Figure 3 provides 3d projections of the pore space of two monoliths – the upper plough horizon and underlying layers. At the used resolution of 200 μm, the uppermost drier and looser layer is diagnosed, where the boundary of change in structure and number of pores between plough horizon and the lower part of natural profile are already clearly visible. The lower subsurface horizons are quite different in pore structure from the upper one (Figure 3).

Based on the tomographic scans, pores in the plough horizon are a uniform mesh made of multidirectional pores and cracks of various diameters. The origin and variety of these voids are explained by the greater susceptibility of this part of the soil profile to transformation both during natural processes of swelling/shrinkage, freezing/thawing, pore and canal formation by plant roots, soil fauna, and as a result of the previous anthropogenic impact – plowing. In contrast, in BE horizon, pores are mostly elongated, rounded, and directed mainly vertically. This explains some results of the previous filtration experiment with KCl for the same monoliths (Shein et al. 2018), when blurring of the motion front in the upper horizon is almost not observed and the dispersion length that describes this blurring is close to classical 5 cm (Tiktak et al. 2000). However, in Ap horizon below the profile, the blurring of the front of opening movement is much more significant due to a quick breakthrough via macropores and dispersion length reaches large values, both according to laboratory experiments with small monoliths 10 cm long and with large monoliths 30 cm long (Shein et al. 2017) and according to field experiments (Shein et al. 2018). And the tomographic 3D picture of the pore space architecture of the middle part of the columns (Figure 3) clearly visualizes these numerical, but indirect characteristics.

However, filtration experiments are carried out by saturated soil. Therefore, it is more appropriate to compare the results of filtration and tomographic studies by saturation of the pore space (Figures 2 and 3). If for E, BE horizons, it is impossible to visually diagnose changes in the pore space structure, then for the plough horizon it is quite clearly noticeable that with natural moisture the soil “crumbles” (a dark mesh of small pores is visible) and has many small cracks, which close after saturation and the monolith looks more complete/continuous (the dark mesh of small pores disappears) (Figure 2).

Description of the pore space was carried out using two variants for processing raster scans of tomographic sections: a simple calculation of scans of individual horizontal projections (2D analysis) and a detailed calculation that combines the processing of raster scans of all projections (3D analysis).

According to the results of 2D analysis, Ap and E-BE horizons differ significantly from each other. The volume of total calculated (i.e., tomographically visible at the

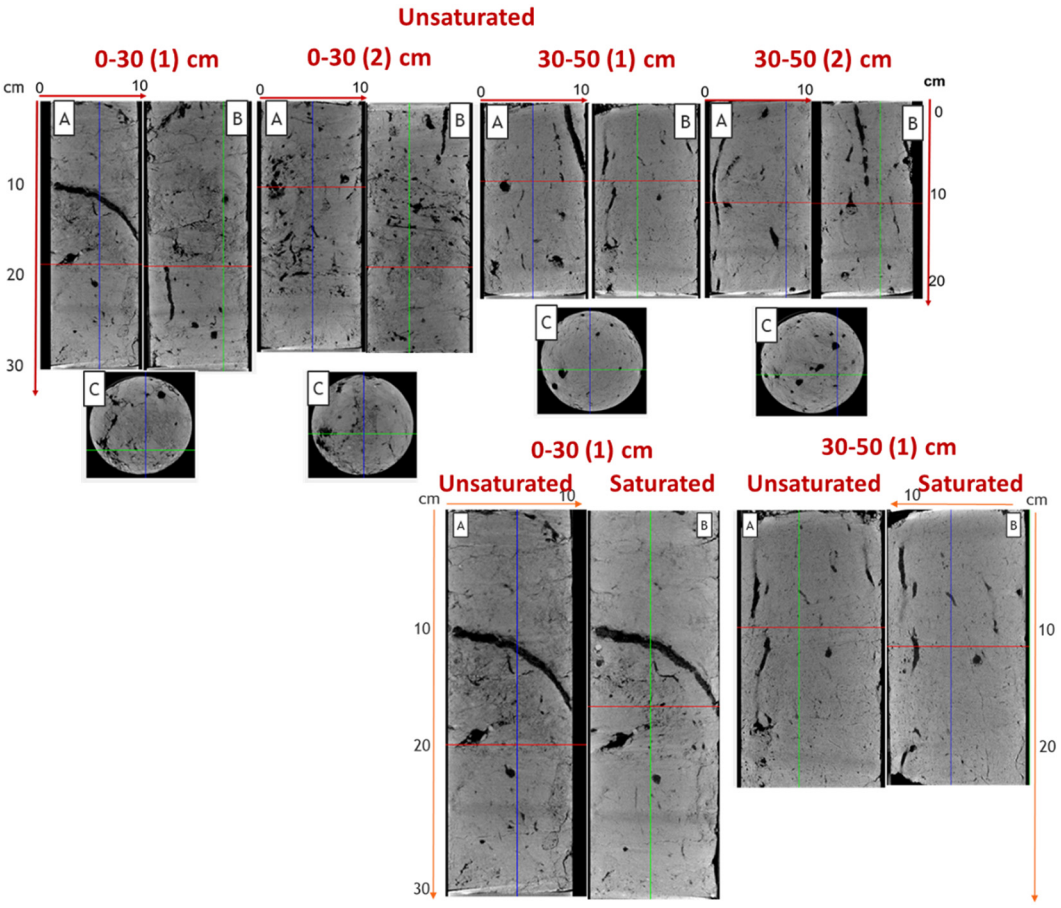

Figure 2: Two-dimensional scans of soil monoliths (projections: A – frontal, B – profile, C – horizontal).

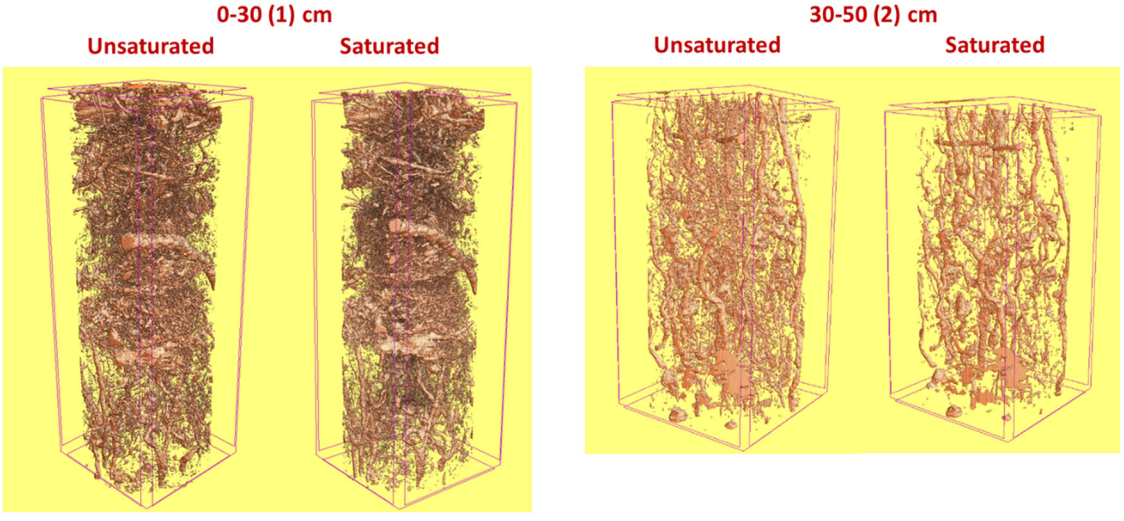

Figure 3: Three-dimensional pore space models before and after saturation.

resolution of 200 µm) pore space for the upper horizon varied between monoliths and was 6.0–7.5%; monoliths from the lower horizons almost did not differ from each other (calculated porosity 2.8–2.9%). At the same time, standard deviation and range indicate a significantly greater variety in sizes and shape of pores in the plough

Table 2: 2D analysis of horizontal projections of tomographic images

Parameter	Monolith			
	0–30 cm (1)	0–30 cm (2)	30–50 cm (1)	30–50 cm (2)
Unsaturated conditions				
Calculated solid phase, %	94.0	92.5	97.1	97.2
Calculated porosity* (mean ± standard devariation):				
closed, %	4.8 ± 2.6	6.4 ± 3.8	2.7 ± 0.7	2.5 ± 0.8
Open, %	1.3 ± 2.4	1.2 ± 1.3	0.9 ± 0.4	0.3 ± 0.3
Total, %	6.0 ± 3.7	7.5 ± 4.1	2.9 ± 0.8	2.8 ± 0.7
Saturated conditions				
Calculated solid phase, %	96.5	95.8	97.1	98.1
Calculated porosity* (mean ± standard devariation):				
closed, %	2.9 ± 1.9	3.8 ± 2.4	2.4 ± 0.6	1.9 ± 0.6
Open, %	0.6 ± 1.4	0.4 ± 0.5	0.2 ± 0.2	0.2 ± 0.2
Total, %	3.5 ± 2.4	4.2 ± 2.5	2.6 ± 0.6	2.1 ± 0.6

*Calculated porosity is a software calculated pore space of soil at a given tomographic resolution (200 μm), which corresponds to a pore size from 1 mm.

horizon. The results obtained on the total porosity are comparable with the studies of agrosoddy-podzolic soil performed several years later when analyzing the whole volume of a monolith 10 cm in diameter and 100 cm in height and even indicate some soil compaction of the fallow over time (Abrosimov et al. 2019). But with the capillary soil saturation with water, there is a general tendency towards a decrease in the proportion of pores associated with the processes of swelling (Table 2).

Diagrams (Figure 4) show comparisons of monoliths for saturated and unsaturated conditions, as well as comparisons of total, open, and closed porosity by swelling. Under saturated conditions for the lower horizons, the calculated porosity decreases by 30%, but reduction

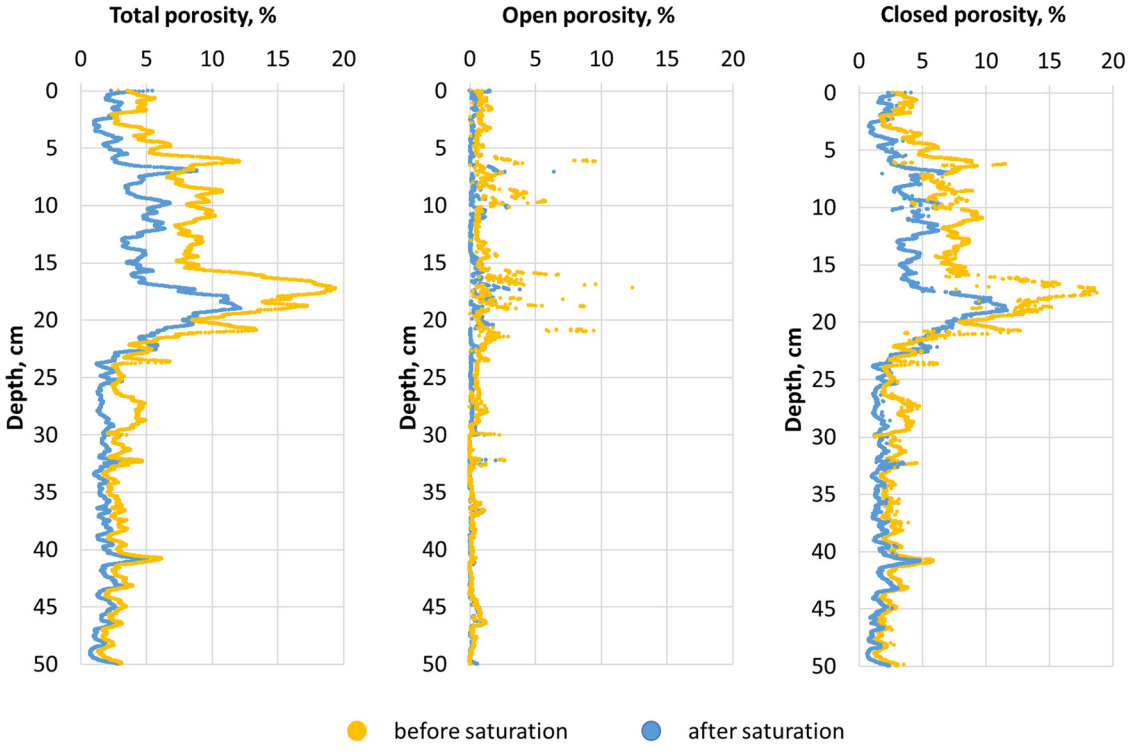

Figure 4: Calculated soil porosity according to 2D analysis.

Table 3: 3D analysis of projections of tomographic images

Calculated parameters	Monoliths			
	0–30 cm (1)	0–30 cm (2)	30–50 cm (1)	30–50 cm (2)
Unsaturated conditions				
Closed porosity, %	0.7	0.8	1.3	0.8
Open porosity, %	6.2	6.9	1.6	2.8
Total porosity, %	6.9	7.7	2.9	3.6
Average pore size, mm	6.2	9.1	7.9	6.5
Number of closed pores	8594	8497	10599	8836
Saturated conditions				
Closed porosity, %	0.7	0.6	0.7	0.7
Open porosity, %	3.5	3.6	1.3	1.2
Total porosity, %	4.2	4.2	2.0	1.9
Average pore size, mm	11.5	10.7	11.7	9.3
Number of closed pores	6736	4329	3656	4114

occurs mainly due to open porosity (22%), while the pore distribution over the layers is uniform (sd = 0.6). For the upper horizon, "peaks" are visible in porosity distribution on the diagram, which indicates large fractures, oriented rather in the horizontal direction. They coincide with the transitions of the soil properties within one horizon (looser upper 10 cm layer, subject to rare harrowing) or at the border of two horizons (plow pan between the old-arable horizon and the submerged one). Herewith, open pores are subject to the greatest volume fluctuations, which can also be seen in 3D analysis. After saturation of the upper horizon, swelling was observed inside the closed pores, but the largest open pores did not completely overlap. Other research papers in the field of microtomography show that intra-aggregate porosity increases by swelling (Skvortsova et al. 2018; Pires et al. 2020); however, the pores of conductive soil area (inter-aggregate), which are discussed here, respond differently to moistening.

Three-dimensional monolith analysis analyzes not individual projections, but the whole monolith (Table 3). Plough and subsurface horizons also differ expressively from each other. It was found that in the upper horizon, the pore space, determined from tomographic scans, is a branched system of pores and cracks and the whole volume of the horizon is involved in migration processes. Monoliths from the lower horizons almost do not differ from each other (total porosity is around 3%) and have mostly rounded vertically oriented pores. Moreover, about 70–85% of the pores visible on tomographic scans make up closed porosity, and the upper horizons have insignificant share of open pores too (about 15–20%).

When saturated, the total porosity in the upper horizon decreased by 39–45%, while the porosity of the subsurface layer decreased by 31–47%, as large vertical pores (root residues) almost do not shrink. However, the pore space structure changed exactly in the underlying horizons, where the ratio of open/closed porosity changed from 55/45% to 65%/35%; the proportion of open pores increased, in contrast to the upper horizon. It is interesting that the process of saturation and swelling of the aggregates did not destroy the pore space, but only increased vertical fracture, and the conducting space of this layer remained the same differentiated. When the saturated soil is stained with brilliant blue dye in the field, you can see the difference in the characteristics of the conducting pore space (Figure 5).

Average pore size (based on the inscribed sphere in 3D analysis) for the upper horizon at natural humidity is slightly higher – 6.2 to 9.1 mm than for the underlying layer – 6.5 to 7.9 mm. When saturated, average diameter for both the upper and lower horizons slightly increases. This is especially noticeable for the lower layer (Table 3). At the same time, for the lower horizon, the number of very small pores and especially large cracks is not as variable as for the upper layer (Figure 6). However, for the upper horizon, a noticeable scatter of pore sizes was observed. Diagram 6 shows a mixture of the peaks towards pore enlargement, which is highly logical because small pores are closed and larger pores and cracks contribute to the average pore size.

Research findings of the pore size distribution were later used to adjust some mathematic models as a part of general work of the All-Russian Research Institute of Phytopathology to create a national scenario for the migration of substances (pesticides, agrochemicals, salts) in soils. In some mathematic models predicting the migration of solutions in soil, the number of macropores in soil

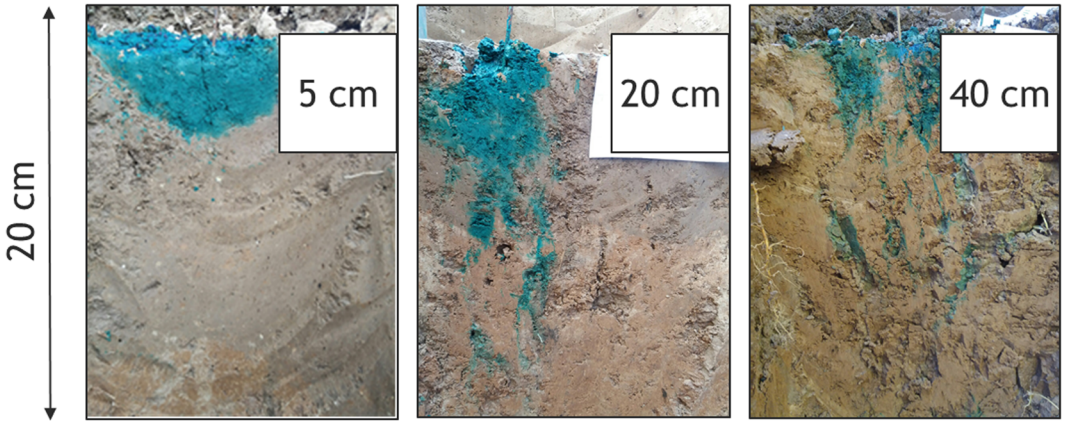

Figure 5: Migration of the marker substance along the soil profile depending on configuration of the conducting pore space.

(MACRO 5.2) or dispersion length parameter (SWAP, PEARL) is required to be entered as an experimental support. For the soils of Moscow region, the option of working with physical support of models, where a mixing step is required, has been studied in sufficient details, but not enough. The number of macropores was set using pedotransfer functions (PTFs), detailed in the literature (Larsbo and Jarvis 2003). However, the model assessment for sensitivity to input parameters showed that increase in the number of macropores in soil can increase soil runoff by up to 10%. Therefore, the content of macropores obtained from tomographic scans and calculated using PTF (Table 4) was compared.

Numerical values of the macroporosity parameters determined from tomographic scans and calculated using pedotransfer functions are close (calculated using PTF, the porosity is less than one third determined from the scans). However, in modeling, it is preferable to use

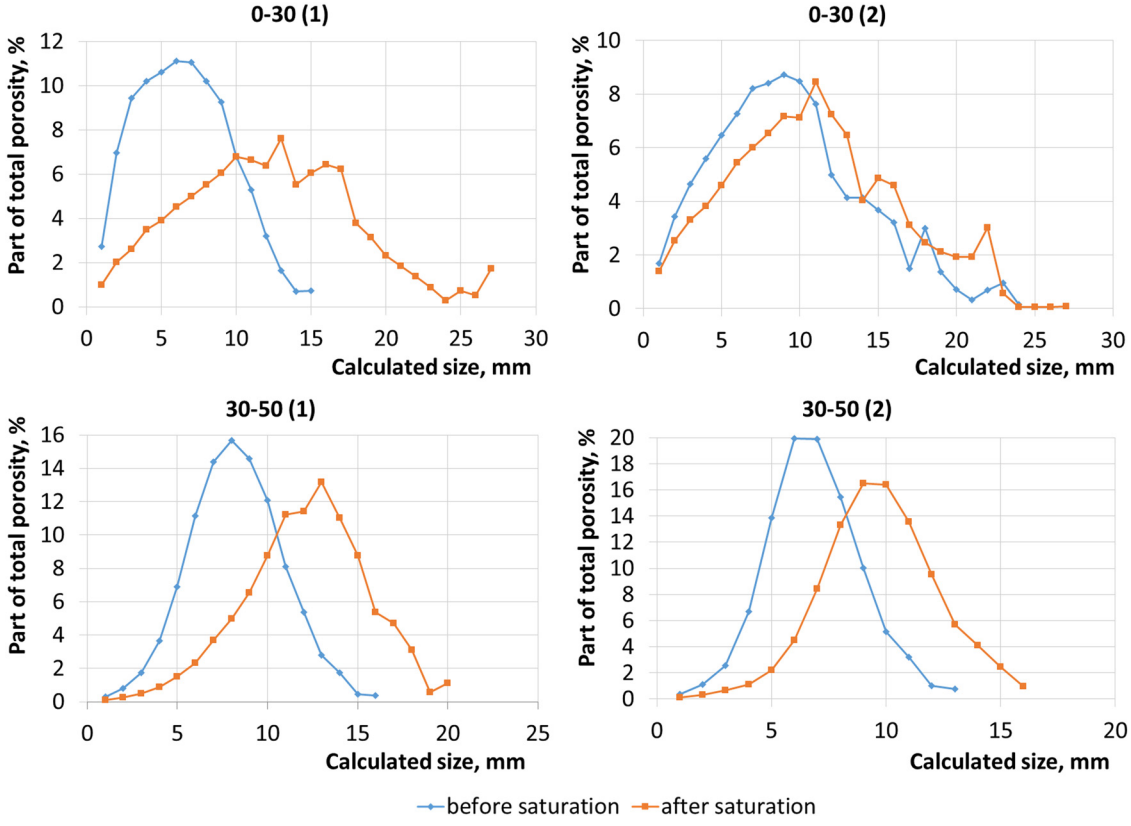

Figure 6: Macropore size distribution before and after saturation.

Table 4: Macroporosity of agrosoddy-podzolic soil obtained from tomographic scans and calculated using PTF

Horizon	Macroporosity, %				
	Tomographic scans (3D analysis)				MACRO 5.2 pedotransfer functions*
	Open (mean)		Total (mean)		
	Unsaturated	Saturated	Unsaturated	Saturated	
Ap	6.6	3.5	7.3	4.2	5.4
E	2.3	1.2	3.3	2.0	2.86
BE					3.23

*Explanation of the calculation algorithm is presented in the model manual.

experimentally confirmed soil characteristics, and then fine-tune according to field experimental data. Thus, a change in the number of macropores from 3% to 10% led to a change in the matter removal up to 20%. However, the result of working with pedotransfer functions in the absence of more accurate data can also be trusted, which will be reflected in the guide to national scenarios.

4 Conclusions

For the soils of the European part of Russia, there is insufficient information on the structure of the largest fraction of the pore space, a quantitative description of which is often required for mathematical prediction of the substance migration in soils. The tomography method showed that the agrosoddy-podzolic soil (Moscow Oblast, Russia) has a heterogeneous architecture of the pore space with an abundance of macropores, which, according to tomography data, are about 7% of the volume of soil monolith for the upper horizon and about 3% for the underlying layer. After saturation, thinner macropores are closed, due to which, against the background of a decrease in the total porosity (up to 4% in the upper horizon and up to 2% in the lower one), the average pore diameter increases (from 6–9 to 10–11 mm). The results obtained will be consistent with the previously received indirect characteristics of preferential migration paths in the soil of this region (staining with a dye, obtaining a dispersion length) and will be used to prepare standard scenarios for migration of substances.

Acknowledgments: This study was supported by the State Project of Russian Scientific-Research Institute of Phytopathology No. 0598-2019-0005 (statement of the problem and object, soil analysis, conceptual generalization), by the Russian Scientific Foundation, project no. 16-16-04014 (performing tomographic studies and determining the physical properties of soils) and by the Faculty of Soil Science, M.V. Lomonosov Moscow State University (citis No. 115122810146 – calculation of tomographic parameters).

Conflict of interest: Authors declare no conflict of interest.

References

[1] Abrosimov KN, Skvorcova EB, Korost DV. Porovoe prostranstvo zalezhnoj dernovo-podzolistoj pochvy moskovskogo regiona: Osobennosti struktury na raznyh ierarhicheskih urovnyah. Vestnik MGPU. Seriya Estestvennye nauki. 2019;2:37–48. doi: 10.25688/2076-9091.2019.34.2.4. (in Russian).

[2] Gorbov SN, Abrosimov KN, Bezuglova OS, Skvortsova EB, Romanenko KA, Tagiverdiev SS. Use of tomographic methods for the study of urban soil properties. In: Vasenev V, Dovletyarova E, Cheng Z, Prokof'eva T, Morel J, Ananyeva N, editors. Urbanization: Challenge and opportunity for soil functions and ecosystem services. SUITMA 2017. Springer Cham: Springer Geography. doi: 10.1007/978-3-319-89602-1_30.

[3] Belik AA, Bolotov AG, Shein EV, Kokoreva AA, Levin AA, Patrushev VYu. Application of neural network pedotransfer functions to calculate soil water retention curve. IOP Conf. Series: Earth and Environmental Science; 2019. p. 368. doi: 10.1088/1755-1315/368/1/012008.

[4] Beulke S, Renaud F, Brown CD. Development of guidance on parameter estimation for the preferential flow model MACRO 4.2. Report to the Department for Environment, Food & Rural Affairs. Silsoe: Cranfield Centre for EcoChemistry; 2002.

[5] Bolotov AG, Shein EV, Makarychev SV. Water retention capacity of soils in the altai region. Eurasian Soil Sc. 2019;52:187–92. doi: 10.1134/S1064229319020030.

[6] Brewer R. Classification of plasmic fabrics of soil materials. In: Jongerius A, editor. Soil Micromorphology. Amsterdam: Elsevier Publ. Co.; 1964. doi: 10.1016/S0166-2481(08)70323-4.

[7] Capowiez Y, Sammartino S, Michel E. Using X-ray tomography to quantify earthworm bioturbation non-destructively in repacked soil cores. Geoderma. 2011;162:124–31. doi: 10.1016/j.geoderma.2011.01.011.
[8] Cercioglu M. Imaging soil pore characteristics using computed tomography as influenced by agroecosystems. Eurasian J Soil Sci. 2018;7(3):195–202. doi: 10.18393/ejss.396237.
[9] Gerke KM, Skvortsova EB, Korost DV. Tomographic method of studying soil pore space: Current perspectives and results for some Russian soils. Eur Soil Sci. 2012;45(7):781–91. doi: 10.1134/S1064229312070034.
[10] Ivanov AL, Shein EV, Skvortsova EB. Tomography of soil pores: From morphological characteristics to structural–functional assessment of pore space. Eurasian Soil Sc. 2019;52(1):50–7. doi: 10.1134/S106422931901006X.
[11] Jarvis N, Koestel J, Larsbo M. Understanding preferential flow in the vadose zone: Recent advances and future prospects. Vadose Zone J. 2016;15:1–11. doi: 10.2136/vzj2016.09.0075.
[12] Jarvis NJ. A review of non-equilibrium water flow and solute transport in soil macropores: Principles, controlling factors and consequences for water quality. Eur J Soil Sci. 2007;58:523–46. doi: 10.1111/j.1365-2389.2007.00915.x.
[13] Kördel W, Klein M. Prediction of leaching and groundwater contamination by pesticides. Pure Appl Chem. 2006;78:1081–90. doi: 10.1351/pac200678051081.
[14] Kuzyakov Y, Blagodatskaya E. Microbial hotspots and hot moments in soil: Concept & review. Soil Biol Biochem 2015;83:184–99. doi: 10.1016/j.soilbio.2015.01.025.
[15] Larsbo M, Jarvis N. MACRO 5.0 A model of water flow and solute transport in microporous soil. Technical description. Swedish: Swedish University of Agricultural Sciences; 2003.
[16] Leue M, Uteau-Puschmann D, Peth S, Nellesen J, Kodešová R, Gerke H. Separation of soil macropore types in three-dimensional X-ray computed tomography images based on pore geometry characteristics. Vadose Zone J. 2019;18:1–13. doi: 10.2136/vzj2018.09.0170.
[17] Mady AY, Shein EV. Assessment of pore space changes during drying and wetting cycles in hysteresis of soil water retention curve in Russia using X-ray computed tomography. Geoderma Regional. 2020;21:e00259. doi: 10.1016/j.geodrs.2020.e00259.
[18] Peyton RL, Gantzer CJ, Anderson SH, Haeffner BA, Pfeifer P. Fractal dimension to describe soil macropore structure using X-ray computed tomography. Water Resour Res. 1994;30(3):691–700. doi: 10.1029/93WR02343.
[19] Pires LF, Auler AC, Roque WL, Mooney SJ. X-ray microtomography analysis of soil pore structure dynamics under wetting and drying cycles. Geoderma. 2020;362:114103. doi: 10.1016/j.geoderma.2019.114103.
[20] Ringrose-Voase AJ. A scheme for the quantitative description of soil macrostructure by image analysis. J Soil Sci. 1987;38:343–56. doi: 10.1111/j.1365-2389.1987.tb02149.x
[21] Rowell D. Pochvovedenie: Metody i ispol'zovanie. Moskva: Kolos; 1998 (in Russian).
[22] Shein EV, Belik AA, Kokoreva AA, Kolupaeva VN, Pletenev PA. Prediction of pesticide migration in soils: The role of experimental soil control. Mosc Univ Soil Sci Bull. 2017;72(4):185–90. doi: 10.3103/S0147687417040044.
[23] Shein EV, Belik AA, Kokoreva AA, Kolupaeva VN. Quantitative estimate of the heterogeneity of solute fluxes using the dispersivity length for mathematical models of pesticide migration in soils. Eurasian Soil Sci. 2018;51(7):797–802. doi: 10.1134/S1064229318070086.
[24] Shein EV. Kurs fiziki pochv: Uchebnoe posobie. Moscow: Izd-vo MGU; 2005 (in Russian.
[25] SHishova LL, Vojtovich NV, editors. Pochvy Moskovskoj oblasti i ih ispol'zovanie T. 1. M. Pochvennyj institut im. V.V. Dokuchaeva; 2002 (in Russian).
[26] Simsek U, Shein EV, Mikailsoy F, Bolotov AG, Erdel E. Subsoil compaction: The intensity of manifestation in silty clayey calcic pantofluvic fluvisols of the Iğdır Region (Eastern Turkey). Eurasian Soil Sc. 2019;52:296–9. doi: 10.1134/S1064229319030104.
[27] Simunek J, Jarvis N, van Genuchten MTh, Gardenas A. Review and comparison of models for describing non-equilibrium and preferential flow and transport in the vadose zone. J Hydrol. 2003;272:14–35. doi: 10.1016/S0022-1694(02)00252-4.
[28] Simunek J, van Genuchten MTh. Modeling nonequilibrium flow and transport processes using HYDRUS. Vadose Zone J. 2008;7(2):782–97. doi: 10.2136/vzj2007.0074.
[29] Skvortsova EB, Shein EV, Romanenko KA, Abrosimov KN, Yudina AV, Klyueva VV, et al. Izmenenie porovogo prostranstva v gumusovyh agregatah dernovo-podzolistoj pochvy pri mnogokratnom zamorazhivanii i ottaivanii. Byulleten' Pochvennogo instituta Im VV Dokuchaeva. 2018;91:6–20. doi: 10.19047/0136-1694-2018-91-6-20 (in Russian).
[30] Skvortsova EB, Shein EV, Romanenko KA, Abrosimov KN. Formation of vesicular pores in aggregates from the eluvial horizon of albic glossic retisol during freeze–thaw cycles. Eurasian Soil Sci. 2020;53(7):913–21. doi: 10.1134/s1064229320070145.
[31] Skvortsova EB, Rozhkov VA, Shchepotev VN, Dmitrenko VN, Tyugai ZN, Khokhlov SF. Variation in the micromorphological indices of pore space in loamy soils of the southern taiga and forest-steppe of European Russia. Eurasian Soil Sci. 2015;48(9):934–45. doi: 10.1134/S1064229315090094.
[32] Smetnik AA, Spiridonov YuYa, Shein EV. Migraciya pesticidov v pochvah. Moskva: RASKHN-VNIIF; 2005 (in Russian).
[33] Tiktak A, van den Berg F, Boesten JJTI, van Kraalingen D, Leistra M, van der Linden AMA. Manual of FOCUS PEARL version 1.1.1. RIVM Report 711401008, Alterra Report 28. Bilthoven, The Netherlands: National Institute of Public Health and the Environment; 2000.
[34] Tuller M, Or D. Preferential flow in structured soils – Hydraulic functions derived from pore-scale processes. 17th World Congress of Soil Science, Bangkok, Thailand; 2002.
[35] Umarova AB, Shein EV, Kukharuk NS. Soil water retention curve of agrogray soils: Influence of anisotropy and the scaling factor. Eurasian Soil Sci. 2014;47(12):1238–44. doi: 10.1134%2FS1064229314120096.
[36] Umarova AB Preimushchestvennye potoki vlagi v pochvah: zakonomernosti formirovaniya i znachenie v funkcionirovanii pochv. M.: GEOS; 2011 (in Russian).
[37] Voronin AD. Osnovy fiziki pochv: Uchebnoe posobie. Moskva: Izd-vo Mosk. un-t; 1986 (in Russian).
[38] Yang Y, Wu J, Zhao S, Zhao S, Han Q, Pan X, et al. Assessment of the responses of soil pore properties to combined soil structure amendments using X-ray computed tomography. Sci Rep. 2018;8:695. doi: 10.1038/s41598-017-18997-1.